

DETECTING ANCIENT SUPERNOVAE AT $Z \sim 5 - 12$ WITH *CLASH*

DANIEL J. WHALEN¹, JOSEPH SMIDT², CLAES-ERIK RYDBERG³, JARRETT L. JOHNSON¹, DANIEL E. HOLZ⁴ AND MASSIMO STIAVELLI⁵

Draft version June 9, 2022

ABSTRACT

Supernovae are important probes of the properties of stars at high redshifts because they can be detected at early epochs and their masses can be inferred from their light curves. Finding the first cosmic explosions in the universe will only be possible with the *James Webb Space Telescope*, the Wide-Field Infrared Survey Telescope and the next generation of extremely large telescopes. But strong gravitational lensing by massive clusters, like those in the *Cluster Lensing and Supernova Survey with Hubble (CLASH)*, could reveal such events now by magnifying their flux by factors of 10 or more. We find that *CLASH* will likely discover at least 2 - 3 core-collapse supernovae at $5 < z < 12$ and perhaps as many as ten. Future surveys of cluster lenses similar in scope to *CLASH* by the *James Webb Space Telescope* might find hundreds of these events at $z \lesssim 15 - 17$. Besides revealing the masses of early stars, these ancient supernovae will also constrain cosmic star formation rates in the era of first galaxy formation.

Subject headings: early universe – galaxies: high-redshift – galaxies: clusters: general – gravitational lensing – large-scale structure of the universe – stars: early-type – supernovae: general

1. INTRODUCTION

In recent years, Type Ia supernovae (SNe) at $z > 0.1$ have been the focus of much attention, and rightly so for their potential to trace cosmic acceleration and constrain the dark energy equation of state. But with the advent of the *James Webb Space Telescope (JWST)* and the next generation of extremely large telescopes, it will soon be possible to detect SNe at the edge of the observable universe at $z \sim 10 - 20$ and use them to probe the earliest stellar populations. These stars are key to the properties of primeval galaxies (Bromm & Yoshida 2011), the origins of supermassive black holes (e.g., Johnson et al. 2012, 2013c; Latif et al. 2013a,b; Schleicher et al. 2013) and the reionization and chemical enrichment of the early intergalactic medium (IGM; Whalen et al. 2004; Beers & Christlieb 2005; Frebel et al. 2005; Joggerst et al. 2010; Ritter et al. 2012; Safranek-Shrader et al. 2013) (for recent reviews, see Whalen 2012; Glover 2013).

Supernovae can reveal the properties of stars at this era because they are visible at high redshifts and their masses can be inferred from their light curves. Recent calculations show that pair-instability (PI) and pulsational pair-instability (PPI) SNe are visible in the near infrared (NIR) at $z \sim 20$ to *JWST* and the Thirty Meter Telescope (TMT) (Joggerst & Whalen 2011; Kasen

et al. 2011; Whalen et al. 2013c; Hummel et al. 2012; Whalen et al. 2013g). These explosions will also be visible at $z \sim 15 - 20$ to the Wide-Field Infrared Survey Telescope (WFIRST) and the Wide-Field Imaging Surveyor for High Redshift (WISH), which could harvest these events in large numbers because of their wide search fields. It is now known that core-collapse (CC) SNe will be detected at $z \sim 10 - 15$ by *JWST*, at $z \sim 7 - 10$ by WFIRST and WISH, and at $z < 7$ by *Euclid* (Whalen et al. 2013d; Meiksin & Whalen 2013). Supermassive SNe (Whalen et al. 2013b; Johnson et al. 2013b; Whalen et al. 2013f,e) and Type II_n SNe (Moriya et al. 2013; Whalen et al. 2013a; Tanaka et al. 2012) will also be visible to these missions at $z \gtrsim 15$.

But could such events be detected in surveys now? In principle, strong lensing by massive galaxy clusters at $z \lesssim 1$ could boost flux from SNe by factors of 10 or more and allow them to be detected at $z \gtrsim 10$ by current instruments. Oguri & Marshall (2010) have estimated detection rates for strongly lensed SNe at low redshifts in future all-sky surveys by the Large Synoptic Survey Telescope (LSST), and Amanullah et al. (2011) have discovered a lensed SN at $z \sim 1.7$ at the edge of the massive galaxy cluster A1689. Many such clusters have now been targeted by the Cluster Lensing and Supernova Survey with *Hubble (CLASH)* to find Type Ia SNe at $z \sim 2$ (Postman et al. 2012). Patel et al. (2013) have already found three SNe at $z < 0.4$ in *CLASH*. The *Hubble Space Telescope (HST)* Frontier Fields program will soon examine six additional cluster lenses to hunt for early galaxies.

We have now calculated the number of SNe that might be discovered at $5 < z < 20$ in *CLASH* and by future cluster surveys by *JWST*. We describe our lens model and derive lensing volumes as a function of redshift in Section 2. In Section 3, we provide NIR light curves for 15 - 40 M_{\odot} CC SNe. Star formation rates at $5 < z < 25$ compiled from gamma-ray burst (GRB) rates, high-

¹ Institute of Cosmology and Gravitation, Portsmouth University, Dennis Sciana Building, Portsmouth PO1 3FX

² Los Alamos National Laboratory, Los Alamos, NM 87545

³ Universität Heidelberg, Zentrum für Astronomie, Institut für Theoretische Astrophysik, Albert-Ueberle-Str. 2, 69120 Heidelberg, Germany

⁴ Enrico Fermi Institute, Department of Physics, and Kavli Institute for Cosmological Physics, University of Chicago, Chicago, IL 60637, USA

⁵ Space Telescope Science Institute, 3700 San Martin Drive, Baltimore, MD 21218

⁶ CCS-2, Los Alamos National Laboratory, Los Alamos, NM 87545

redshift galaxy luminosity functions, and numerical simulations are presented in Section 4. In Section 5, these rates are convolved with lensing volumes and SN luminosities to determine the rates at which SNe will be found by a single cluster lens as a function of redshift. We conclude in Section 6.

2. LENSING MODEL

In lieu of actual lensing maps for each cluster (Zitrin et al. 2009), which are not yet available for *CLASH*, we model a cluster lens as a singular isothermal sphere whose magnification, μ , is uniquely specified by its Einstein radius, θ_E . We use equations 4 - 6 from Pan & Loeb (2013) to compute the area in the source plane that is magnified above a given μ with cosmological parameters from the most recent Planck+WP+highL+BAO data: $\Omega_M = 0.308$ and $\Omega_\Lambda = 0.692$ (Planck Collaboration et al. 2013). Lensing volumes as a function of μ and z for $\theta_E = 35$ and 55 arcsec are plotted in Fig. 1. These two radii bracket θ_E for 5 of the 25 clusters selected for *CLASH* and are typical of clusters with high μ (the other 20 cluster lenses in the survey have $\theta_E \sim 10 - 30$ arcsec). Note that lensing volumes decrease with redshift above $z \sim 2$ because the luminosity distance D_A peaks and begins to fall above this redshift. This trend, plus the fact that star formation rates plummet at high z as we show later, are the two greatest limitations to using cluster lenses to detect early SNe.

Real clusters are better described by Navarro-Frenk-White (NFW) profiles. To check the validity of the SIS approximation, we have redone the analysis of Pan & Loeb (2013) with NFW halos. Although the SIS has a very simple lensing distribution, the NFW lens is somewhat more complicated because there are two critical curves instead of just one, which leads to infinite magnification at a finite radius in the source plane and at the origin (the latter is also true of the SIS). We have solved the general lensing equation in the source plane for a range of lens and source redshifts, determining the locations of the images and calculating μ for each one. Our calculations show that spherical NFW profiles have slightly larger magnifications than SIS profiles for an equivalent Einstein angle. Our SIS lensing volumes should therefore be taken to be lower limits.

3. SN LIGHT CURVES

In Fig. 2 we show H band light curves for 15 - 40 M_\odot Population III (Pop III) CC SNe at $z = 7$ and 10 in the *HST* Wide-Field Camera 3 (WFC3) 1.63 μm filter, whose sensitivity limit is \sim AB mag 27.3 for total exposure times of a few 10^5 s. These explosions are designated by progenitor type (z-series are explosions of red supergiant stars), mass (15, 25 and 40 M_\odot) and energy (B, D, and G are 0.6, 1.2 and 2.4×10^{51} erg) (Whalen et al. 2013d). Our SNe and spectra were modeled with the Los Alamos RAGE and SPECTRUM codes (Frey et al. 2013). The spectra were then cosmologically redshifted, dimmed, and convolved with absorption by the neutral IGM and *HST* and *JWST* filter response functions to obtain NIR light curves.

What mostly determines the light curve of a CC explosion is its energy and the internal structure of the star. Rotational and convective mixing lead to similar structures for zero- and solar-metallicity stars of equal

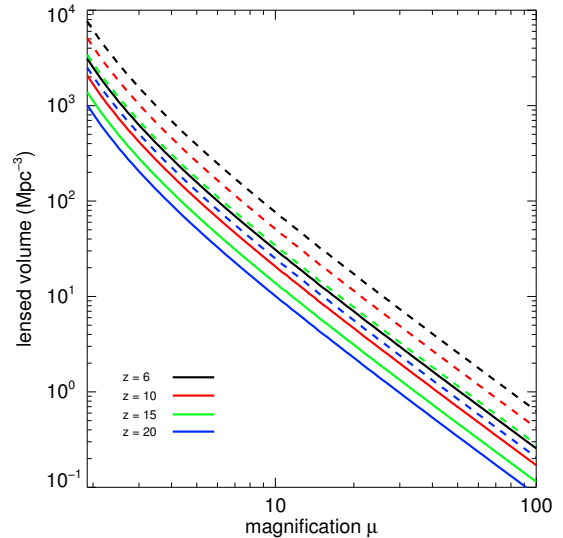


FIG. 1.— Volumes lensed by magnifications greater than μ , plotted as a function of μ for 35 arcsec (solid) and 55 arcsec (dashed) cluster lenses.

mass. Because the energy of the SN depends on the entropy profile of the core of the star prior to explosion, it also does not vary strongly with metallicity (see Fig. 1 of Whalen & Fryer 2012). Furthermore, at zero metallicity most 15 - 40 M_\odot stars are thought to die as red supergiants because of internal mixing over their lives. For these reasons, our light curves are likely to be representative of CC SNe over all the redshifts in our study, not just the earliest epochs. We consider only CC SNe because PI and Type II_n SNe need little or no magnification to be seen by *CLASH* and they are much less frequent than Type II SNe.

Unlike the fiducial 15 M_\odot CC SN in Pan & Loeb (2013), our SNe have H band fluxes that can be detected by *CLASH* with only moderate $\mu = 10 - 20$ at $5 < z < 12$. At $z = 15$ there is essentially no flux at 1.63 μm so *HST* would not detect Type II events above this redshift. At $z = 15$ they are brightest in the 2.77 μm *JWST* NIR-Cam filter, as shown in Fig. 2. At this redshift, three of the SNe exceed the NIRCcam detection limit of AB mag 32 without being lensed, and μ of only $\sim 2 - 5$ are required to boost the others above this limit. Only modest magnifications would be required to boost the z15B, z15D, z15G, z40D and z40G explosions above the detection limit for *JWST* at $z = 20$, so a cluster lens could in principle reveal CC SNe from this epoch. But small lensing volumes and low star formation rates above $z \sim 13$ make it unlikely that a cluster survey would encounter such events, as we discuss below.

4. HIGH-REDSHIFT STAR FORMATION RATES

We show star formation rates (SFRs) inferred from the luminosity functions of early galaxies (Campisi et al. 2011), from GRB rates (Ishida et al. 2011; Robertson & Ellis 2012), and from numerical simulations (Wise et al. 2012; Johnson et al. 2013a; Pawlik et al. 2013; Xu et al. 2013; Hasegawa & Semelin 2013; Muratov et al. 2013) for $5 < z < 25$ in Fig. 3 (see Tornatore et al. 2007; Trenti & Stiavelli 2009, for other SFRs from simulations that fall within the range shown here). The SFRs from early

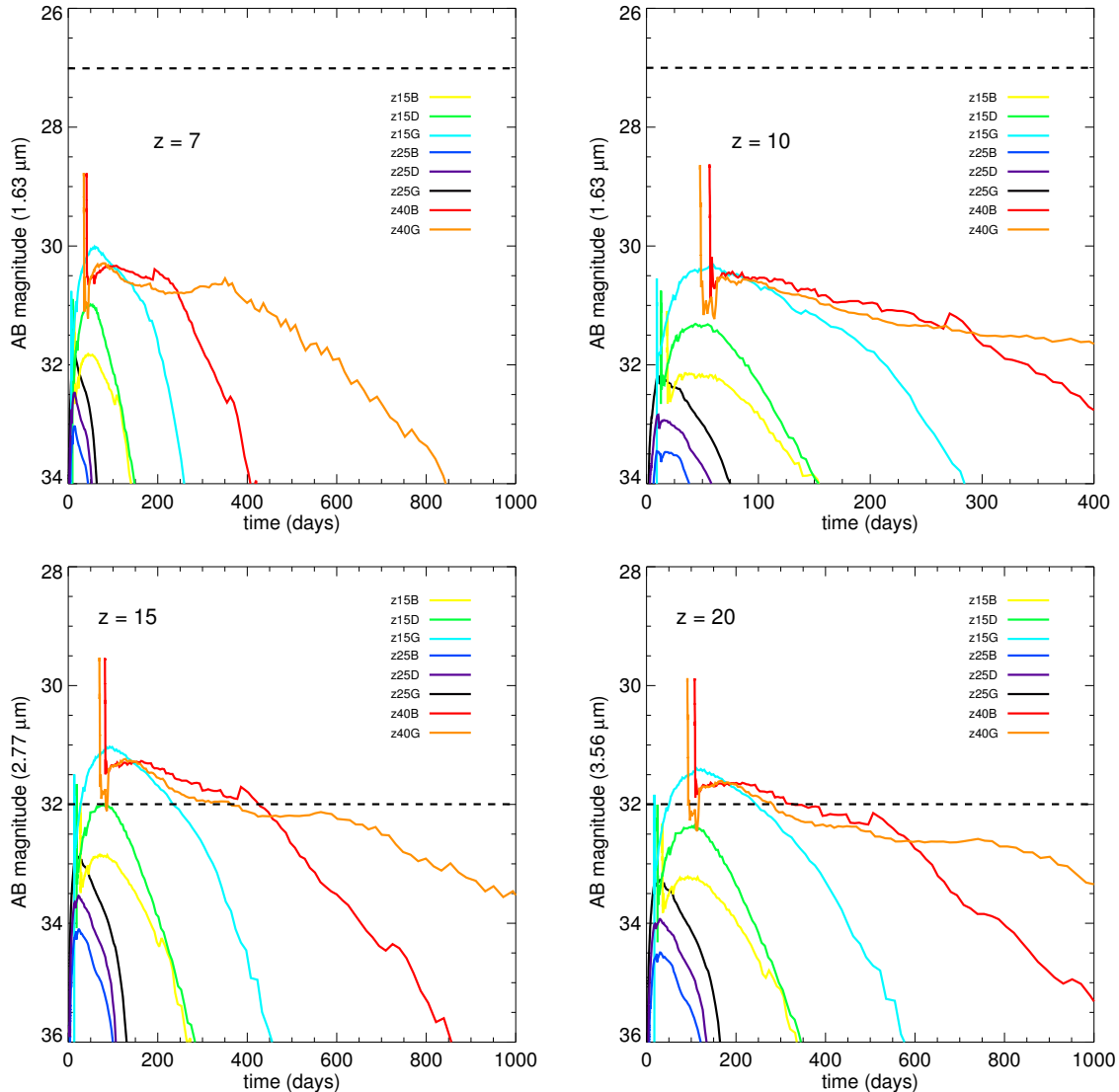


FIG. 2.— *CLASH* ($1.63 \mu\text{m}$) and *JWST* NIRCcam (2.77 and $3.56 \mu\text{m}$) light curves for $15 - 40 M_{\odot}$ Pop III CC SNe at $z = 7, 10, 15,$ and 20 . The *JWST* filters shown are those in which the SN is brightest at that redshift. Times on the x -axes are in the observer frame. The dashed horizontal lines at AB mag 27 and 32 are *CLASH* and *JWST* detection limits, respectively.

galaxies exclude the steep faint end slopes of low luminosity galaxies and are likely lower than the true rates. The SFRs from Robertson & Ellis (2012) and Ishida et al. (2011) above $z \sim 5 - 7$ are mostly extrapolated from those at lower redshifts. For SFRs above $z \sim 15$ we must rely entirely upon simulations.

SFRs from GRBs vary by $\sim 50\%$ at $z = 5$ and by a factor of 10 at $z = 15$. The rates from early galaxies vary by the similar factors over the same redshifts, with an overall spread in SFR between the two methods of a factor of ~ 400 at $z = 15$. The rates predicted by numerical simulations also vary by about two orders of magnitude from $z \sim 10 - 25$. The SFRs in most of these models are just those in a few protogalaxies in their simulation volumes and are therefore subject to small box statistics. The simulations also include a variety of feedback processes that lead to a wide range of evolution in stellar populations over cosmic time. We sample this broad range of

SFRs with three fits. On the low end is the dashed line in Fig. 3 that borders the simulations with the lowest SFRs from below. As a middle case, we take the dashed line through the simulations with the higher SFRs down to $z = 15$, where it intersects with the GRB rates, and then adopt the GRB rates down to $z = 5$. As an upper case, we take the upper dashed line down to $z \sim 12$, where the SFR is $0.2 M_{\odot} \text{ yr}^{-1} \text{ Mpc}^{-3}$, and then level off the SFR at this rate down to $z = 5$. This rate is equal to SFRs inferred from both GRBs and SN measurements at $z \sim 3$ (for the latter, see Strolger et al. 2004), and is a conservative upper limit.

5. SN SNAPSHOT RATES

The SN rate can be derived from the cosmic SFR if the initial mass function (IMF) and upper and lower mass limits for CC SN production are known. By $5 < z < 12$, most stars form in young galaxies in which metals and dust are produced, so we adopt the Salpeter IMF and the

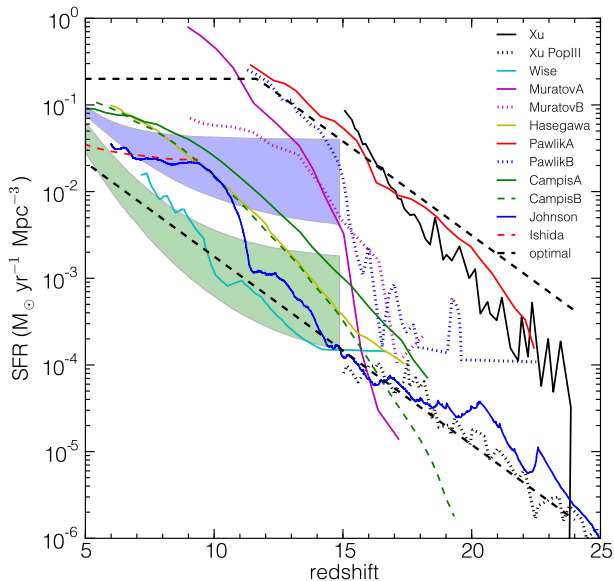


FIG. 3.— SFRs over cosmic time. The blue and green bands are rates inferred from GRBs (Ishida et al. 2011; Robertson & Ellis 2012) and luminosities of high z protogalaxies (Campisi et al. 2011), respectively. The SFRs compiled from numerical simulations are from Wise et al. (2012); Johnson et al. (2013a); Pawlik et al. (2013); Hasegawa & Semelin (2013); Xu et al. (2013); Muratov et al. (2013). The two dashed lines are mean and upper fits to the simulation SFRs. The Xu Pop III SFR is for Pop III stars only, the others are total Pop III + II SFRs.

usual rule of thumb of ~ 1 SN / $100 M_{\odot}$ of stars formed for this mass distribution. This IMF underestimates the SN rate above $z \sim 12$ because a greater fraction of SF likely goes into stars above $20 M_{\odot}$, so our SN rates should be taken as lower limits. We have verified that our choice of SN rate per solar mass does not vary by more than a factor of two for reasonable choices of upper and lower masses for CC SNe and our IMF. This is far less than the uncertainty in the cosmic SFR itself, which is up to a factor of ~ 400 . For simplicity, we also take the 3 or 4 brightest of our SNe to represent CC SNe at high redshift in general.

If SFR is the rate of star formation observed today and dt is the cadence, or time between observations of a given cluster, the rate and time between observations at redshift z are $\text{SFR} (1+z)$ and $dt/(1+z)$, respectively. The number of SNe enclosed by the lensing volume $dV(z, \mu)$ whose flux is boosted by a factor μ or more at redshift z over the time dt in the observer frame is then

$$dN(z, \mu) = \text{SFR} (1+z) \frac{1 \text{ SN}}{100 M_{\odot}} dV(z, \mu) \frac{dt}{1+z}. \quad (1)$$

To obtain the total number of SNe above a given redshift $N(> z)$ whose flux would be boosted above *CLASH* or *JWST* detection limits, we integrate Eq. 5 over all z above that redshift and all μ above the minimum magnification needed to detect the event at each redshift. We assume an average cadence $dt = 3$ months and take μ_{min} to be ~ 10 for *CLASH* at $5 < z < 12$ for our SNe because their peak AB magnitudes do not evolve strongly over this range. We assume $\mu_{min} \sim 2$ for $5 < z < 20$ for

JWST as a conservative estimate, since even at $z \sim 20$ some of the SNe do not have to be lensed to be detected. The total number of SNe that would be found by 35 and 55 arcsec lenses in *CLASH* and by *JWST* are plotted in the left and right panels of Fig. 4, respectively. The SFRs used in each plot are designated by "hi" (high), "med" (medium), and "low" (low), the three fits described at the end of Section 4. We include curves for $\mu = 20$ for *CLASH* and for $\mu = 5$ for *JWST* to consider dimmer events.

For (very) low SFRs, the number of SNe that *CLASH* would detect in both lenses is too small to appear on these plots. For the medium rates at $\mu = 10$, the 35 and 55 arcsec lenses would find 0.08 and 0.2 SNe, respectively, or 1 - 3 events total above $z = 5$. For the high rates, the two lenses would detect 0.2 and 0.5 SNe, or 3 - 9 events at $z > 5$ in the entire survey. If all the SNe at this epoch were dimmer events that require magnifications of 20 to be seen, at most one or two would be detected by *CLASH*. The practical limit to CC SN detections with *CLASH* is $z \sim 12 - 13$; above these redshifts, the number of SNe that either lens would detect is too low for any to appear in the survey, even at high SFRs. However, at SFRs that are between the medium and high rates, one or two SNe in the survey could be $z \sim 10 - 12$ events. The total number of CC SNe that may be found in *CLASH* is similar to the number of PI SNe that might be found by *JWST* at $z \sim 20$ over its mission life (Hummel et al. 2012).

Future cluster surveys by *JWST* that are similar in scope to *CLASH* will detect far greater numbers of CC explosions at $5 < z < 12$. For the medium SFRs at $\mu = 2$, the 35 and 55 arcsec lenses would detect 18 and 40 events each. Unlike *CLASH*, *JWST* would detect events even at the lowest SFRs: at $\mu = 2$, the two lenses could observe 1.5 and 3 SNe each. Even 1 - 2 dimmer events would appear in such surveys at these rates. Furthermore, *JWST* would find 1 - 3 CC SNe at $z \sim 15 - 17$, almost the era of first star formation.

6. CONCLUSION

Although primordial SNe won't be discovered prior to the arrival of *JWST*, WFIRST and the next generation of extremely large telescopes, our calculations show that *CLASH* may already have found a few SNe (and perhaps up to 10) at $5 < z < 12$, redshifts well above those at which SNe have been found to date ($z = 3.9$; Cooke et al. 2012). Such detections could probe the properties of stars in the first galaxies and constrain the cosmic SFR at $5 < z < 12$ to within the uncertainty of the IMF over this interval, which is much smaller. Even the failure to detect SNe in *CLASH* would be useful because it would place upper limits on SFRs at $5 < z < 12$ by ruling out the models with the highest rates. Our results argue for the use of longer cadences in future surveys of cluster lenses, both to capture more events and more easily identify explosions with slowly evolving luminosities as transients. Any doubt over whether a particular event is actually a SN could easily be resolved by additional observations of that cluster.

Future surveys by *JWST* that are similar in scope to *CLASH* could discover hundreds of SNe out to $z \sim 15 - 17$, but not at higher redshifts because event rates are so low and the lensing volumes with the μ needed to reveal

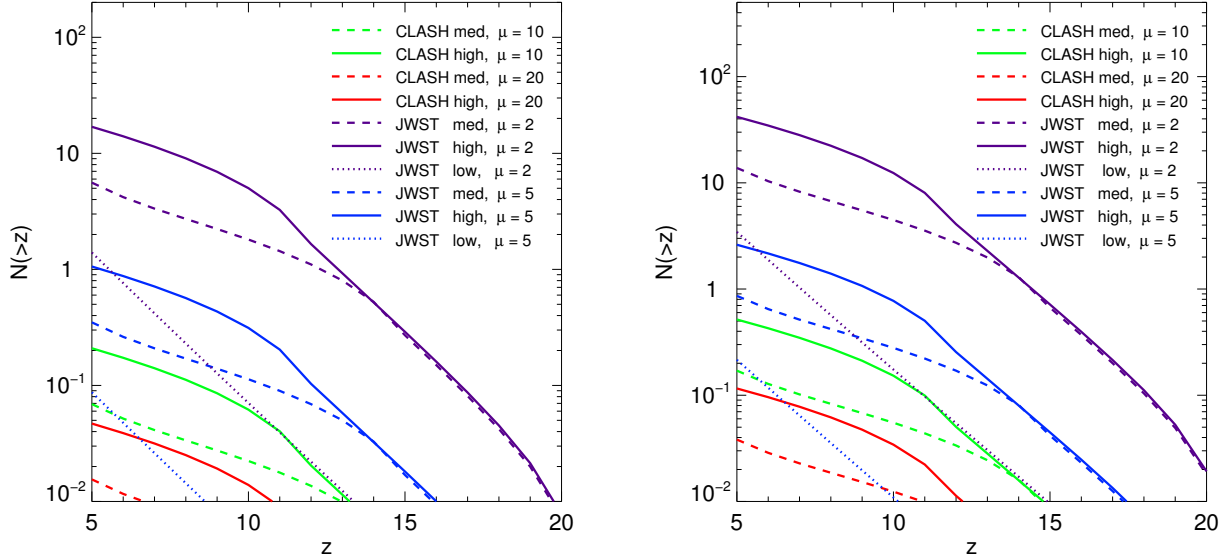


FIG. 4.— The number of SNe detected above a redshift z by a single 35 arcsec lens (left) and a 55 arcsec lens (right) in *CLASH* and by *JWST*.

the SNe are so small. An alternate approach might be to exploit the strong lensing of events everywhere on the sky at some redshift by all the structures below that redshift in future wide-field surveys. Far greater volumes at high redshifts could be lensed in this manner than by galaxy clusters, albeit at lower average magnifications, and compensate for the low SFRs at $z \gtrsim 15$. This approach would be ideally suited to future all-sky campaigns by WFIRST and WISH. It is not yet known if the lower peak μ in all-sky lensing, which are due to the smaller masses of lenses at high z , will be sufficient to boost flux from ancient SNe above the detection thresholds of these missions. Calculations are now underway to determine if strong lensing

in all-sky surveys will open yet another window on the primordial universe.

DJW thanks Utte Rydberg and Michele Trenti for helpful discussions in the course of work. He was supported by the Baden-Württemberg-Stiftung by contract research via the programme Internationale Spitzenforschung II (grant P-LS-SPII/18). JS was supported by a LANL Director's Postdoctoral Fellowship. Work at LANL was done under the auspices of the National Nuclear Security Administration of the U.S. Dept of Energy at Los Alamos National Laboratory under Contract No. DE-AC52-06NA25396.

REFERENCES

- Amanullah, R., Goobar, A., Clément, B., Cuby, J.-G., Dahle, H., Dahlén, T., Hjorth, J., Fabbro, S., Jönsson, J., Kneib, J.-P., Lidman, C., Limousin, M., Milvang-Jensen, B., Mörtzell, E., Nordin, J., Paech, K., Richard, J., Riehm, T., Stanishev, V., & Watson, D. 2011, *ApJ*, 742, L7
- Beers, T. C. & Christlieb, N. 2005, *ARA&A*, 43, 531
- Bromm, V. & Yoshida, N. 2011, *ARA&A*, 49, 373
- Campisi, M. A., Maio, U., Salvaterra, R., & Ciardi, B. 2011, *MNRAS*, 416, 2760
- Cooke, J., Sullivan, M., Gal-Yam, A., Barton, E. J., Carlberg, R. G., Ryan-Weber, E. V., Horst, C., Omori, Y., & Díaz, C. G. 2012, *Nature*, 491, 228
- Frebel, A., Aoki, W., Christlieb, N., Ando, H., Asplund, M., Barklem, P. S., Beers, T. C., Eriksson, K., Fechner, C., Fujimoto, M. Y., Honda, S., Kajino, T., Minezaki, T., Nomoto, K., Norris, J. E., Ryan, S. G., Takada-Hidai, M., Tsangarides, S., & Yoshii, Y. 2005, *Nature*, 434, 871
- Frey, L. H., Even, W., Whalen, D. J., Fryer, C. L., Hungerford, A. L., Fontes, C. J., & Colgan, J. 2013, *ApJS*, 204, 16
- Glover, S. 2013, in *Astrophysics and Space Science Library*, Vol. 396, *Astrophysics and Space Science Library*, ed. T. Wiklund, B. Mobasher, & V. Bromm, 103
- Hasegawa, K. & Semelin, B. 2013, *MNRAS*, 428, 154
- Hummel, J. A., Pawlik, A. H., Milosavljević, M., & Bromm, V. 2012, *ApJ*, 755, 72
- Ishida, E. E. O., de Souza, R. S., & Ferrara, A. 2011, *MNRAS*, 418, 500
- Joggerst, C. C., Almgren, A., Bell, J., Heger, A., Whalen, D., & Woosley, S. E. 2010, *ApJ*, 709, 11
- Joggerst, C. C. & Whalen, D. J. 2011, *ApJ*, 728, 129
- Johnson, J. L., Dalla, V. C., & Khochfar, S. 2013a, *MNRAS*, 428, 1857
- Johnson, J. L., Whalen, D. J., Even, W., Fryer, C. L., Heger, A., Smidt, J., & Chen, K.-J. 2013b, arXiv:1304.4601
- Johnson, J. L., Whalen, D. J., Fryer, C. L., & Li, H. 2012, *ApJ*, 750, 66
- Johnson, J. L., Whalen, D. J., Li, H., & Holz, D. E. 2013c, *ApJ*, 771, 116
- Kasen, D., Woosley, S. E., & Heger, A. 2011, *ApJ*, 734, 102
- Latif, M. A., Schleicher, D. R. G., Schmidt, W., & Niemeyer, J. 2013a, *MNRAS*, 433, 1607
- 2013b, *MNRAS*, 430, 588
- Meiksin, A. & Whalen, D. J. 2013, *MNRAS*, 430, 2854
- Moriya, T. J., Blinnikov, S. I., Tominaga, N., Yoshida, N., Tanaka, M., Maeda, K., & Nomoto, K. 2013, *MNRAS*, 428, 1020
- Muratov, A. L., Gnedin, O. Y., Gnedin, N. Y., & Zemp, M. 2013, *ApJ*, 773, 19
- Oguri, M. & Marshall, P. J. 2010, *MNRAS*, 405, 2579
- Pan, T. & Loeb, A. 2013, *MNRAS*

- Patel, B., McCully, C., Jha, S. W., Rodney, S. A., Jones, D. O., Graur, O., Merten, J., Zitrin, A., Riess, A. G., Matheson, T., Sako, M., Holoien, T. W.-S., Postman, M., Coe, D., Bartelmann, M., Balestra, I., Benitez, N., Bouwens, R., Bradley, L., Broadhurst, T., Cenko, S. B., Donahue, M., Filippenko, A. V., Ford, H., Garnavich, P., Grillo, C., Infante, L., Jouvel, S., Kelson, D., Koekemoer, A., Lahav, O., Lemze, D., Maoz, D., Medezinski, E., Melchior, P., Meneghetti, M., Molino, A., Moustakas, J., Moustakas, L. A., Nonino, M., Rosati, P., Seitz, S., Strolger, L. G., Umetsu, K., & Zheng, W. 2013, ArXiv e-prints
- Pawlik, A. H., Milosavljević, M., & Bromm, V. 2013, ApJ, 767, 59
- Planck Collaboration, Ade, P. A. R., Aghanim, N., Armitage-Caplan, C., Arnaud, M., Ashdown, M., Atrio-Barandela, F., Aumont, J., Baccigalupi, C., Banday, A. J., & et al. 2013, arXiv:1303.5076
- Postman, M., Coe, D., Benítez, N., Bradley, L., Broadhurst, T., Donahue, M., Ford, H., Graur, O., Graves, G., Jouvel, S., Koekemoer, A., Lemze, D., Medezinski, E., Molino, A., Moustakas, L., Ogaz, S., Riess, A., Rodney, S., Rosati, P., Umetsu, K., Zheng, W., Zitrin, A., Bartelmann, M., Bouwens, R., Czakon, N., Golwala, S., Host, O., Infante, L., Jha, S., Jimenez-Teja, Y., Kelson, D., Lahav, O., Lazkoz, R., Maoz, D., McCully, C., Melchior, P., Meneghetti, M., Merten, J., Moustakas, J., Nonino, M., Patel, B., Regös, E., Sayers, J., Seitz, S., & Van der Wel, A. 2012, ApJS, 199, 25
- Ritter, J. S., Safrank-Shrader, C., Gnat, O., Milosavljević, M., & Bromm, V. 2012, ApJ, 761, 56
- Robertson, B. E. & Ellis, R. S. 2012, ApJ, 744, 95
- Safrank-Shrader, C., Milosavljevic, M., & Bromm, V. 2013, arXiv:1307.1982
- Schleicher, D. R. G., Palla, F., Ferrara, A., Galli, D., & Latif, M. 2013, arXiv:1305.5923
- Strolger, L.-G., Riess, A. G., Dahlen, T., Livio, M., Panagia, N., Challis, P., Tonry, J. L., Filippenko, A. V., Chornock, R., Ferguson, H., Koekemoer, A., Mobasher, B., Dickinson, M., Giavalisco, M., Casertano, S., Hook, R., Blondin, S., Leibundgut, B., Nonino, M., Rosati, P., Spinrad, H., Steidel, C. C., Stern, D., Garnavich, P. M., Matheson, T., Grogin, N., Hornschemeier, A., Kretchmer, C., Laidler, V. G., Lee, K., Lucas, R., de Mello, D., Moustakas, L. A., Ravindranath, S., Richardson, M., & Taylor, E. 2004, ApJ, 613, 200
- Tanaka, M., Moriya, T. J., Yoshida, N., & Nomoto, K. 2012, MNRAS, 422, 2675
- Tornatore, L., Ferrara, A., & Schneider, R. 2007, MNRAS, 382, 945
- Trenti, M. & Stiavelli, M. 2009, ApJ, 694, 879
- Whalen, D., Abel, T., & Norman, M. L. 2004, ApJ, 610, 14
- Whalen, D. J. 2012, arXiv:1209.4688
- Whalen, D. J., Even, W., Lovekin, C. C., Fryer, C. L., Stiavelli, M., Roming, P. W. A., Cooke, J., Pritchard, T. A., Holz, D. E., & Knight, C. 2013a, ApJ, 768, 195
- Whalen, D. J., Even, W., Smidt, J., Heger, A., Chen, K.-J., Fryer, C. L., Stiavelli, M., Xu, H., & Joggerst, C. C. 2013b, ApJ, 778, 17
- Whalen, D. J. & Fryer, C. L. 2012, ApJ, 756, L19
- Whalen, D. J., Fryer, C. L., Holz, D. E., Heger, A., Woosley, S. E., Stiavelli, M., Even, W., & Frey, L. H. 2013c, ApJ, 762, L6
- Whalen, D. J., Joggerst, C. C., Fryer, C. L., Stiavelli, M., Heger, A., & Holz, D. E. 2013d, ApJ, 768, 95
- Whalen, D. J., Johnson, J. L., Smidt, J., Heger, A., Even, W., & Fryer, C. L. 2013e, ApJ, 777, 99
- Whalen, D. J., Johnson, J. L., Smidt, J., Meiksin, A., Heger, A., Even, W., & Fryer, C. L. 2013f, ApJ, 774, 64
- Whalen, D. J., Smidt, J., Even, W., Woosley, S. E., Heger, A., Stiavelli, M., & Fryer, C. L. 2013g, arXiv:1311.1221
- Wise, J. H., Turk, M. J., Norman, M. L., & Abel, T. 2012, ApJ, 745, 50
- Xu, H., Wise, J. H., & Norman, M. L. 2013, ApJ, 773, 83
- Zitrin, A., Broadhurst, T., Rephaeli, Y., & Sadeh, S. 2009, ApJ, 707, L102